INDIAN JOURNAL OF SCIENCE AND TECHNOLOGY

RESEARCH ARTICLE

FTIR Spectroscopy and Microstructural Study of Fe Doped Calcium Copper Titanate (CCTO)

Sachin Tripathi[1]*, Seema Srivastava[1], Vishal Singh Chandel[2,3], Ameer Azam[4], Upendra Kumar Mishra[5,3]

1 Department of Physics, Integral University, Lucknow, 226026, Uttar Pradesh, India
2 Department of Applied Science and Humanities, Rajkiya Engineering College, Ambedkar Nagar, 224122, Uttar Pradesh, India
3 Dr. A.P.J. Abdul Kalam Technical university, Lucknow, 226031, Uttar Pradesh, India
4 Department of Physics, Faculty of science, Islamic University of Madinah Al Jamiah, Madinah, 42351, Saudi Arabia
5 Department of Applied Science, Shri Ramswaroop Memorial College of Engineering and Management, Lucknow, 226028, Uttar Pradesh, India

OPEN ACCESS

Received: 25-08-2023

Accepted: 05-06-2024

Published: 18-06-2024

Citation: Tripathi S, Srivastava S, Chandel VS, Azam A, Mishra UK (2024) FTIR Spectroscopy and Microstructural Study of Fe Doped Calcium Copper Titanate (CCTO). Indian Journal of Science and Technology 17(25): 2570-2576. https://doi.org/10.17485/IJST/v17i25.2170

* **Corresponding author**.

sachhintripathi@gmail.com

Funding: None

Competing Interests: None

Published By Indian Society for Education and Environment (iSee)

ISSN
Print: 0974-6846
Electronic: 0974-5645

Abstract

Objectives : The analysis of present material is to reveal the effect of Fe atom by replacing the Ti atom in CCTO for chemical properties. **Methods:** Pure and Fe doped $CaCu_3Ti_{4-x}Fe_xO_{12}$ (x=0.05, 0.10, and 0.15) CCTO ceramics were synthesized by solid-state reaction route and calcination was done at 930°C for 12 hrs with heating rate of 4°C/min. The phase structure of samples was confirmed by X-ray Diffraction (XRD) and found single phase calcium copper titanate. Morphology of all samples was investigated by scanning electron microscopy. Absorption band have been also recorded for all samples. **Findings:** The structure remains cubic by doping of Fe atom in place of Ti atom. The average size of all the samples were lies between 1-1.3μm. **Novelty:** The bond strength becomes stronger as the doping of Fe atom takes place. The large absorption band is found in the range 380-700 cm^{-1}. The peak of large band is shifted towards lower wave number. These higher wavelengths can be used in water pollutants. The increased volume size of samples shows lower energy band gap. This lower energy band gap enhanced the electrical properties.

Keywords: FESEM; XRD; FTIR; EDS; CCTO

1 Introduction

In the field of electronics, the demand is increasing, and the problems of energy are becoming a global issue as science and technology develops[(1)]. Titanium dioxide (TiO_2)[(2)], barium titanate ($BaTiO_3$)[(3)], strontium titanate ($SrTiO_3$)[(4)], calcium copper titanate ($CaCu_3Ti_4O_{12}$/CCTO)[(5)] are some of the main material types to be employed in a large amount for electrical applications. Although considerable progress has been made in developing these dielectric materials, the main challenges are still low energy

storage density and high loss of electrons.

The substrate known as a photocatalyst is essential to the process of photocatalysis, which removes pollutants from the environment by using light to speed up the required chemical reactions [6]. The nano-catalyst of calcium copper titanate, derived from mineral industry waste, has shown promising results in reducing pollution problems and increasing energy economy [7]. Its ability to efficiently adsorb a wide range of contaminants, such as heavy metal ions, dyes, and organic molecules, makes calcium copper titanate an effective and versatile tool for water pollutant removal. Due to its lower cost, increased capacity, and use of environmentally safe and green methods, photocatalysis has attracted a lot more interest for the degradation of pollutants [8]. There are several benefits and uses for the narrow energy band gap. Large band gap materials can be employed as RF signal processing or power switching applications [9]. In this manner more transition metals doping are very much helpful to develop the properties of CCTO. In the present study, the doping of Fe atom in pure CCTO has been done.

In this work, undoped $CaCu_3Ti_4O_{12}$ and $CaCu_3Ti_{4-x}Fe_xO_{12}$(x = 0.05, 0.10, 0.15) are abbreviated as CCTO and CCTFO respectively, were prepared by solid-state reaction route at same sintering and calcination conditions. X-ray diffraction (XRD), energy dispersive X-ray spectroscopy (EDS), scanning electron microscopy (SEM) and Fourier transform infrared spectroscopy (FTIR) were employed to reveal properties of the microstructure, size, and absorption bands.

2 Materials and Method

Pure calcium copper titanate (CCTO ceramic) has been synthesized from highly pure precursors calcium carbonate ($CaCO_3$, Thomas Baker, Purity $\geq$ 99%), copper oxide (CuO, Thomas Baker, Purity $\geq$ 99%) AR grade and titanium (IV) oxide (TiO_2, Sigma Aldrich, Purity 99.5%) powder (size<100nm).

Firstly, by using the appropriate calculation, stoichiometric amount of materials have been mixed with the help of agate mortar. The mixture was dried at 100°C for 2 hrs. After that the powder was calcined at 930°C for 12 hrs (heating/cooling rate of 4°C/min) in a programmable furnace.

$$CaCO_3 + 3CuO + 4TiO_2 \xrightarrow{930^\circ C} CaCu_3Ti_4O_{12} + CO_2 \uparrow$$

In a similar way, the process of synthesis was repeated to obtain the composition of $CaCu_3Ti_{4-x}Fe_xO_{12}$ ceramics by doping of Fe content in x= 5%, 10% and 15% proportions.

$$CaCO_3 + 3CuO + 3.95TiO_2 + 0.025Fe_2O_3 \xrightarrow{930^\circ C} CaCu_3Ti_{3.95}Fe_{0.05}O_{12}$$

$$CaCO_3 + 3CuO + 3.90TiO_2 + 0.05Fe_2O_3 \xrightarrow{930^\circ C} CaCu_3Ti_{3.90}Fe_{0.10}O_{12}$$

$$CaCO_3 + 3CuO + 3.85TiO_2 + 0.075Fe_2O_3 \xrightarrow{930^\circ C} CaCu_3Ti_{3.85}Fe_{0.15}O_{12}$$

The phase confirmation was done by PAN analytical X-ray diffraction (XRD) with Cu-K_α radiation in the 2θ range of 20° to 80° with scan rate of 5°/min. The peak matching has to be done by using XRD analysis. The surface morphology was evaluated by scanning electron microscopy (SEM, Nova NanoSEM 450) and FTIR.

3 Results and Discussions

3.1 X-ray Diffraction

Table 1. Lattice parameter and unit volume cell of all samples

S.No.	Sample name	Lattice parameter (Å)	Unit volume cell (Å^3)
1.	$CaCu_3Ti_4O_{12}$	7.3875	403.1
2.	$CaCu_3Ti_{3.95}Fe_{0.05}O_{12}$	7.389	403.41
3.	$CaCu_3Ti_{3.90}Fe_{0.10}O_{12}$	7.3935	404.15
4.	$CaCu_3Ti_{3.85}Fe_{0.15}O_{12}$	7.3940	404.23

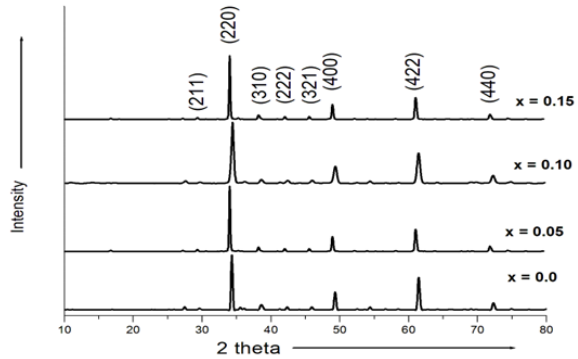

Fig 1. XRD pattern of pure CCTO and Fe doped CCTO at x= 5%, 10% and 15%

XRD patterns of un-doped CCTO ($CaCu_3Ti_4O_{12}$) and Fe doped CCTO ($CaCu_3Ti_{4-x}Fe_xO_{12}$) samples sintered at 930°C for 12 h are shown in Figure 1. It confirms the pure CCTO has single phase and structure remains cubic by doping of Fe content in CCTO ceramics. It is reported that Fe^{3+} ion is more appropriate at the place of Ti site than Cu site in CCTO[10]. The CCTO structure was determined by using X-ray diffraction (XRD, PAN analytical) with Cu K_α (λ = 1.5406 Å) as radiation source (40KV, scan rate 4°/min). The peak fitting, phase identification of XRD profile were examined by powderX software. Table 1 shows the increase in doping % of Fe leads to increase the volume size of the materials.

The crystalline size (τ) of the pure and Fe doped ceramics has been evaluated by using the Scherrer's formula:

$$\tau = \frac{k\lambda}{\beta\, cos\theta}$$

Where k is the shape coefficient (k= 0.9), λ is the X-ray wavelength used in XRD, β is the full width at half maximum (FWHM) of each phase obtained from powderX software and θ is the diffraction angle. The crystallite sizes of all the samples are calculated by Debye-Scherrer and modified Scherrer equation are listed in the Table 2. The crystallite sizes of the samples are increased by increase in doping amount of Fe. The Williamson Hall plan has revealed the strain in the materials. Table 3 shows the micro-strain of the samples based on the slope of 4sinθ and βcosθ values[11–13]. At 5% Fe doping, the sample exhibits large increase in the micro strain which further slightly increases.

Table 2. Crystallite size from Scherrer's and modified Scherrer's equation

Samples	Calcination (°C)	Debye–Scherrer equation size (in nm)	Modified Scherrer equation size (in nm)
$CaCu_3Ti_4O_{12}$	930°C	30.1233202	37.12800194
$CaCu_3Ti_{3.95}Fe_{0.05}O_{12}$		31.27440483	40.28629974
$CaCu_3Ti_{3.90}Fe_{0.10}O_{12}$		31.33125577	40.0057479
$CaCu_3Ti_{3.85}Fe_{0.15}O_{12}$		31.33926466	40.29314899

Table 3. Crystallite size, micro-strain and dislocation density by Williamson-Hall plot

Samples	Calcination (°C)	Williamson Hall plot size (in nm)	Micro strain (e)	Dislocation Density (δ)
$CaCu_3Ti_4O_{12}$	930°C	48.27213333	0.0908848	0.11020323
$CaCu_3Ti_{3.95}Fe_{0.05}O_{12}$		57.92656	0.110	0.101817492
$CaCu_3Ti_{3.90}Fe_{0.10}O_{12}$		57.89236264	0.111074	0.102011218
$CaCu_3Ti_{3.85}Fe_{0.15}O_{12}$		58.15919679	0.111	0.102240248

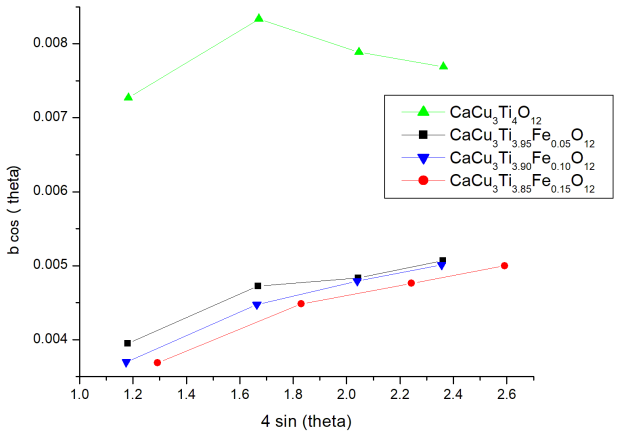

Fig 2. Williamson-Hall plot of CCTO and Fe doped CCTO at x= 5%, 10% and 15%

3.2 FE-SEM (Field Effect Scanning Electron Microscopy) Analysis:

The surface morphology of pure and Fe doped CCTO at different concentration has been seen by FE-SEM micrographs in Figure 3 **(a-d)**. It is confirmed that pure CCTO has cubic structure and atoms are arranged precisely in regular manner. The grains are formed uniformly with the average size of about 1.0-1.3μm but smaller grains lie in the range of 0.4-0.6μm. The cubic shape remains same as the doping of Fe has been done at different concentrations. Fe doped CCTO (5%, 10%, and 15%) have larger grains size of about 1μm but the size of smaller grains was lying in the range of 0.2-0.3μm[14]. The smaller grains of Fe doped samples are relatively less than the pure CCTO. It is well defined that Fe^{3+} ions take well place at the Ti^{4+} ions. As the doping is increased the size of the larger grains has been decreased.

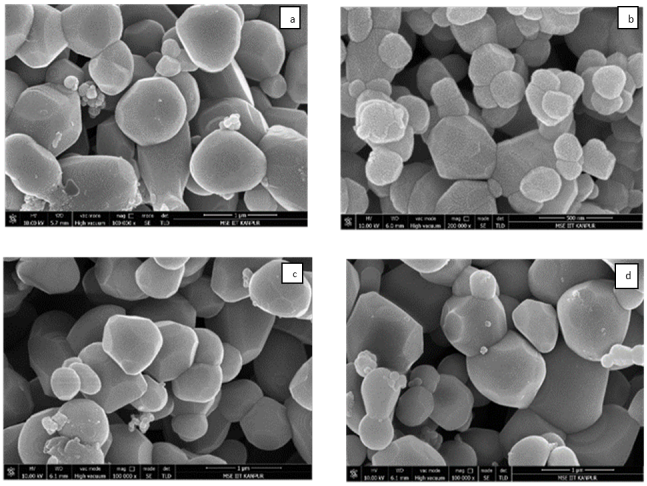

Fig 3. FE-SEM images of pure (a) and Fe (b) 5%, (c) 10%, (d) 15% doped samples

3.3 EDS (Energy Dispersive Spectra)

EDS analysis has been used to analyze the presence of elements in CCTO. It also confirms the weight (wt %) percent of each element. EDS shows that the different concentration of Fe doping in the pure CCTO and gives the weight of each substance. During the EDS analysis different areas of pure and doped cermaics were focused and equivalent peaks are shown in Figure 4

(a-d). Peak of carbon element has been observed because sample was deposited carbon tape. Because of this it is clearly seen that weight of carbon element is neglected. The EDS spectra gives information of Ca, Cu, Ti element for pure ceramic and weight of Fe element with Ca, Cu, Ti for doped samples. The quantity of Ca, Cu and Ti were 6.15, 24.63 and 62.55 respectively. The atomic % were also listed for all elements of the powder synthesized samples.

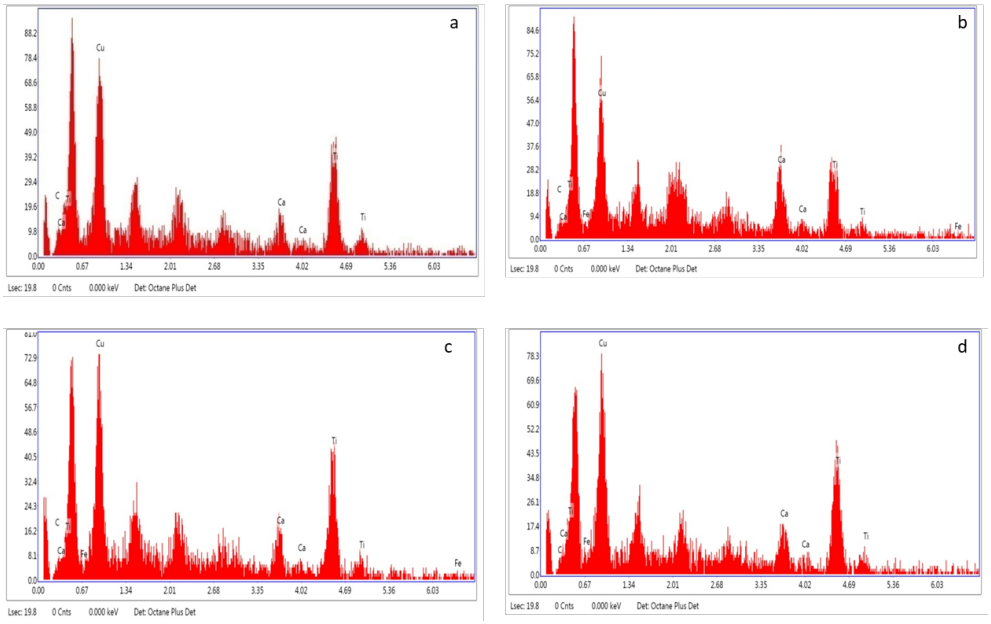

Fig 4. a. EDS image of Fe doped CCTO at x=0%, b. EDS image of Fe doped CCTO at x=5%, c. EDS image of Fe doped CCTO at x=10%, d. EDS image of Fe doped CCTO at x=15%

3.4 FTIR Spectroscopy

Figure 5 shows FT-IR spectra of pure and Fe doped CCTO samples calcined at 930°C with doping concentration of 5%, 10% and 15% respectively.

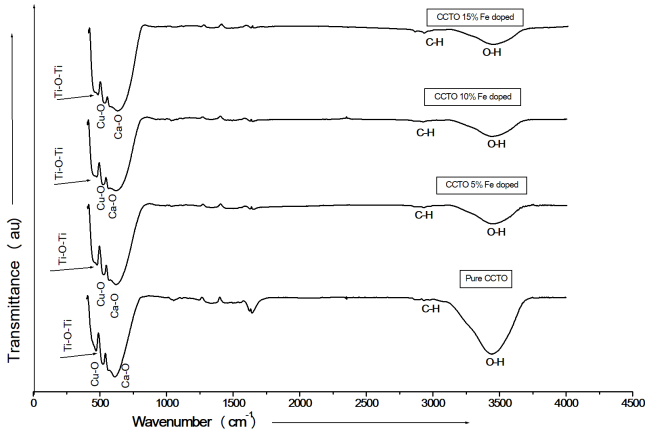

Fig 5. FTIR spectra of Pure and Fe doped CCTO

The absorption peak at 460 cm^{-1} is corresponding to Ti-O-Ti bond. The wave number 525 cm^{-1} is corresponding to Cu-O stretching. The Ca-O bending is observed at 615 cm^{-1}. The absorption peak at 2938 cm^{-1} is corresponding to very strong C-H stretching. The large peak at 3431 cm^{-1} is due to prevalence of O-H stretching[15]. The wave number 380-700 cm^{-1} shows the absorption band of TiO_6 prevailing in the CCTO structure. The peaks of O-H bond shifted towards left which means the bond strength becomes more stable and strong[16–18]. The 15% doping of Fe sample shows more stability. This will help in enhanced the photo catalytic activity of CCTO.

4 Conclusions

All the pure and Fe doped samples are synthesized by using solid precursors $CaCO_3$, CuO, TiO_2 and Fe_2O_3. The XRD analysis confirms all peaks of CCTO as reported with given lattice parameter and mean crystalline size. The lattice parameter of Pure CCTO is less than Fe doped samples of CCTO. The SEM analysis revealed the information about cubic structure of samples and their grain size lies between 0.2-0.3μm which is very much comfortable for solid state reaction method. The weight % of each element in pure CCTO found with the help of EDS study. FTIR analysis confirms the absorption band 380-700 cm^{-1} is due to TiO_6 prevailing of CCTO structure. The absorption band is shifted towards the lower wavelength. It shows the 15% iron doped CCTO is increased the photocatalytic activity of sample.

Acknowledgment

Authors are thankful to the Research and Development of Integral University, Lucknow for providing the research facilities and manuscript communication number IU/R&D/2024-MCN0002756.

References

1) Jayakrishnan AR, Silva J, Kamakshi K, Dastan D, Annapureddy V, Pereira M, et al. Are lead-free relaxor ferroelectric materials the most promising candidates for energy storage capacitors? *Progress in Materials Science*. 2023;132:1–33. Available from: https://doi.org/10.1016/j.pmatsci.2022.101046.
2) Parangi T, Mishra MK. Titanium Dioxide as Energy Storage Material: A Review on Recent Advancement. In: Ali HM, editor. Titanium Dioxide - Advances and Applications. IntechOpen. 2021. Available from: https://www.intechopen.com/chapters/77775.
3) Sun J, Yan G, Fang B, Zhao X, Zhang S, Lu X, et al. Improving energy storage performance of barium titanate-based ceramics by doping MnO2. *Journal of Energy Storage*. 2024;78. Available from: https://doi.org/10.1016/j.est.2023.110007.
4) Liu L, Liu Y, Hoa J, Chen J, Li P, Chen S, et al. Multi-scale collaborative optimization of SrTiO3-based energy storage ceramics with high performance and excellent stability. *Nano Energy*. 2023;109. Available from: https://doi.org/10.1016/j.nanoen.2023.108275.
5) Kawrani S, Boulos M, Cornu D, Bechelany M. From Synthesis to Applications: Copper Calcium Titanate(CCTO) and its Magnetic and Photocatalytic Properties. *Chemistry open*. 2019;8(7):922–950. Available from: https://doi.org/10.1002/open.201900133.
6) Saravanan A, Kumar PS, Jeevanantham S, Anubha M, Jayashree S. Degradation of toxic agrochemicals and pharmaceutical pollutants: Effective and alternative approaches toward photocatalysis. *Environmental Pollution*. 2022;298. Available from: https://doi.org/10.1016/j.envpol.2022.118844.
7) Makhoul E, Boulos M, Cretin M, Lesage G, Miele P, Cornu D, et al. CaCu3Ti4O12 Perovskite Materials for Advanced Oxidation Processes for Water Treatment. *Nanomaterials*. 2023;13(14):1–29. Available from: https://doi.org/10.3390/nano13142119.
8) Ma G, Hisatomi T, Domen K. Semiconductors for photocatalytic and photoelectrochemical solar water splitting. In: From Molecules to Materials . Springer, Cham. 2015;p. 1–56. Available from: https://doi.org/10.1007/978-3-319-13800-8_1.
9) Alam N, Khatoon T, Chandel VS, Azam A. Band Gap Engineering in Zinc Doped Sodium Hexa-titanate. *Indian Journal of Science and Technology*. 2019;12(21):1–5. Available from: https://dx.doi.org/10.17485/ijst/2019/v12i21/143934.
10) Zhuk NA, Lutoev VP, Lysyuk AY, Makeev BA, Belyy VA, Nekipelov SV, et al. Thermal behavior, magnetic properties, ESR, XPS, Mössbauer and NEXAFS study of Fe-doped CaCu3Ti4O12 ceramics. *Journal of Alloys and Compounds*. 2021;855(Part 1). Available from: https://doi.org/10.1016/j.jallcom.2020.157400.
11) Mishra UK, Chandel VS, Singh OP, Alam N. Effect of Calcination Temperature on Soot Oxidation Activity by Pure and La-doped CeO2 (Ce1-xLaxO2) Synthesized via Orange Peel Extract. *Iranian Journal of Science*. 2024;48:585–597. Available from: https://doi.org/10.1007/s40995-024-01612-0.
12) Mishra UK, Chandel VS, Singh OP, Alam N. Synthesis of CeO2 and Zr-Doped CeO2 (Ce1−xZrxO2) Catalyst by Green Synthesis for Soot Oxidation Activity. *Arabian Journal for Science and Engineering*. 2023;48:771–777. Available from: https://doi.org/10.1007/s13369-022-06997-x.
13) Mishra UK, Chandel VS, Singh OP, Alam N, Sharma AK. Effect of La co-doping in Zr-doped CeO2 (LaxZr0.05Ce1-(x+0.05)O2) catalyst synthesized via orange peel extract for soot oxidation. *Ionics*. 2024;30:509–519. Available from: https://doi.org/10.1007/s11581-023-05273-8.
14) Kumari N, Meena S, Rathore D, Singhal R, Dwivedi UK. Study of dielectric properties of CaCu3Ti4O12 synthesized via different routes: Effect of sintering temperature. *Ceramics International*. 2023;49(2):2549–2556. Available from: https://doi.org/10.1016/j.ceramint.2022.09.234.
15) Jesurani S, Kanagesan S, Velmurugan R, Kalaivani T. Phase formation and high dielectric constant of calcium copper titanate using sol-gel route. *Journals of Materials Science: Materials of Electronics*. 2012;23:668–674. Available from: https://doi.org/10.1007/s10854-011-0468-9.
16) Alam N, Khatoon T, Chandel VS, Azam A, Rashmi. Comparative Analysis of Sodium Hexa-titanate (Na2Ti6O13) & Sodium-Potassium Hexa-titanate (Na1.5K0.5Ti6O13). In: International Conference on Multifunctional Materials (ICMM-2019) ;vol. 1495 of Journal of Physics: Conference Series. 2020;p. 1–6. Available from: https://iopscience.iop.org/article/10.1088/1742-6596/1495/1/012034.
17) Khatoon T, Alam N, Chandel VS, Azam A, Srivastava S, Gupta J. Exploring the synergistic effects of La3+ substitution on dielectric performance of manganese cobalt ferrite: Implications for advanced electronic applications. *Ceramics International*. 2024;50(4):7156–7167. Available from: https://doi.org/10.1016/j.ceramint.2023.12.083.

18) Khatoon T, Chandel VS, Alam N, Azam A, Srivastava S, Khan S. La3+ substituted Ni0.5 Co0.5 Fe2 O4 nanoferrites: Magnetically separable catalysts for sunlight-driven photo-oxidative degradation of Methylene Blue. *Journal of Alloys and Compounds*. 2023;961. Available from: https://doi.org/10.1016/j.jallcom.2023.171125.